Japanese Journal of Applied Physics
47(2), 1234–1237(2008)

Controlling Open-Circuit Voltage of Organic Photovoltaic Cells by Inserting Thin Layer of Zn-Phthalocyanine at Pentacene/C_{60} Interface

Yoshiki Kinoshita, Taku Hasobe, and Hideyuki Murata*

Japan Advanced Institute of Science and Technology (JAIST),

1-1 Asahi-dai, Nomi, Ishikawa 923-1292, Japan

*E-mail address: murata-h@jaist.ac.jp

We demonstrate organic photovoltaic cell composed of multi charge-separation (MCS) interfaces in the active layer for the improvement of power conversion efficiency (η_P). The MCS interfaces are composed of pentacene/C_{60} and Zn-phthalocyanine (ZnPc)/C_{60} by inserting thin layer of ZnPc at the CS interface between pentacene/C_{60}. We obtain enhanced η_P and V_{oc} in accordance with the increased energy difference between the lowest unoccupied molecular orbital (LUMO) level of the n-type material (C_{60}) and the HOMO level of the p-type material (ZnPc). By inserting 2 nm ZnPc at the interface, both open-circuit voltage (V_{oc}) and short-circuit current density (J_{sc}) have been improved simultaneously and the resulting η_P reaches 2.07%.

KEYWORDS: multi charge separation (MCS) interfaces, V_{oc} and J_{sc} controlled independently

1. Introduction

In recent years attention has been drawn toward solar energy conversion to develop inexpensive renewable energy sources. New concepts and approaches for production of efficient and low-cost organic solar cells have been desired for the further development and application. So far, the power conversion efficiency (η_P) has steadily improved through the use of new materials and device structures.[1-13] In particular, great efforts have been made for the enhancement of short-circuit current density (J_{sc}). An approach to increase the J_{sc} is use of molecules with high carrier mobilities.[4,7] One of the representative materials is pentacene, and the photovoltaic cells using pentacene as the p-type layer attains high η_P values.[4] The other one is use of bulk heterojunctions (e.g., the composite of p- and n-type materials) as an active layer in both polymer and small molecule-based solar cells.[8-13]

In the bulk heterojunction cells, the distance that an exciton must travel from its generation site to charge-separation (CS) interface is reduced by the formation of interpenetrating network of p- and n-type materials. This leads to a higher J_{sc} owing to the enhanced exciton diffusion length.[13] Thus, the formation of the proper interpenetrating network in an active layer is a key for the improvement of J_{sc}, which governs the final conversion efficiency: η_P. However, in these composite cells, it is quite challenging to precisely control the formation of interpenetrating network by solely fabrication process such as annealing condition. Furthermore, there is no enhancement effect of open-circuit voltage (V_{oc}) due to the formation of interpenetrating network. In other word, for the further improvement of η_P, it is essential to enhance V_{oc}, with maintaining the corresponding J_{sc}.

In this study, we demonstrate new type organic photovoltaic cells composed of multi

charge separation (MCS) interfaces, as shown Fig. 1, which can be controlled V_{oc} and J_{sc} independently. The device consists of charge separation interfaces based on pentacene/C_{60} and Zn-phthalocyanine (ZnPc)/C_{60} in which pentacene and ZnPc are employed as the p-type molecules to form p-n junction with n-type of C_{60}. Highest occupied molecular orbital (HOMO) level of those p-type materials are 5.0 eV (pentacene)[14] and 5.1~5.17 eV (ZnPc).[14,15] By inserting thin layer of ZnPc at the CS interface between pentacene/C_{60}, we obtained enhanced η_P and V_{oc} in accordance with the increased energy difference between the lowest unoccupied molecular orbital (LUMO) level of the n-type material and the HOMO level of the p-type material.[5,16,17] By inserting 2 nm ZnPc at the CS interface, both J_{sc} and V_{oc} have been improved simultaneously and the resulting η_P reaches 2.07%.

In addition, we have investigated series resistance (R_s) and shunt resistance (R_{sh}) as a function of the film thickness ZnPc at the CS interface between pentacene/C_{60}. R_s is attributed to the bulk resistivity of the semiconducting materials, the contact resistance between the semiconductors and the adjacent electrodes, and the resistance associated with probe lines and interconnections. On the other hand, R_{sh} takes into account the loss of carriers via the leakage paths that may be created, for example, through pinholes in the film. To obtain a high fill factor for efficient η_P, R_s approaching zero and R_{sh} approaching infinity is desirable.[18]

2. Experimental

Devices were fabricated on a glass substrate coated with indium–tin–oxide (ITO) electrode. The thickness of ITO was 150 nm and the sheet resistance was 8.2 Ω/sq. Devices consisted of pentacene as p-type layer with high hole mobility, ZnPc as a

p-type material with large HOMO level (5.1~5.17 eV)[14,15], C_{60} as n-type layer, and bathocuproine (BCP) as an exciton blocking layer. Pentacene and ZnPc were purchased from Aldrich, and C_{60} was purchased from MTR.. Pentacene, ZnPc and C_{60} were sublimed in our laboratory before use. High purity materials of and BCP were provided by Nippon Steel Chemical and were used without further purification. All organic layers were deposited onto the ITO substrate by vacuum evaporation using Knudsen-cells under 10^{-6} Torr. The device structure are ITO / pentacene (50 nm) / ZnPc (x nm) / C_{60} (40 nm) / BCP (10 nm) / Ag (100 nm) as shown Fig. 1. The thickness of the ZnPc layer was changed from 0 nm to 10 nm. The Ag electrode was deposited onto the BCP layer through a shadow mask. All organic layers and cathode layers were successively fabricated by vacuum evaporation in the chamber. η_P were estimated from current density–voltage (J-V) characteristics under simulated solar light (AM1.5, 100 mW/cm^2) irradiation. J-V characteristic was measured using a source meter (Keithley SMU2400) at room temperature in nitrogen atmosphere.

3. Results and Discussion

Figures 2(a) and 2(c) show the current density–voltage (J-V) characteristics and values of J_{sc} and V_{oc} as a function of the thickness of ZnPc layer under the illumination of AM 1.5 (100 mW/cm^2) simulated solar light. We observe monotonic increase of V_{oc} from 0.39 V to 0.53 V in the 0 - 10 nm range corresponding to that the larger HOMO level of ZnPc up to 5.17eV compared with pentacene (5.0 eV) [Fig. 2(b)]. The increase of V_{oc} from 0.39 V to 0.53 V is corresponding to the increase in HOMO energy difference from ZnPc to pentacene. On the other hand, the J_{sc} reaches maximum (9.0 mA/cm^2, V_{oc}=0.40 V) at 1 nm of ZnPc film thickness, then it rapidly decreases in the 3 -

6 nm range. The both V_{oc} and J_{sc} are approximately unchanged in the 6 - 10 nm range of ZnPc layer. Figure 2(d) shows η_P relative to the ZnPc layer thickness. The maximum η_p attains 2.07% in ITO/pentacene (50 nm)/ ZnPc (2 nm)/C_{60} (40 nm)/BCP (10 nm)/Ag (100 nm), which is higher than 1.83% of the device without ZnPc layer; ITO/pentacene (50 nm)/C_{60} (40 nm)/BCP (10 nm)/Ag (100 nm).

Figure 3(a) shows the photocurrent action spectra as a function of the thickness of ZnPc. The two peaks at 590 and 670 nm are derived from pentacene, whereas a broad response in 700 - 800 nm region is originated from ZnPc layer [Fig. 3(b)]. The device with 2-nm-thick ZnPc layer shows η_{EQE} spectrum corresponding to the absorption of ZnPc (700 - 800 nm) in addition to that of pentacene (λ_{peak}= 580 and 670 nm). These results demonstrate that the charge separation at the interface of ZnPc/C_{60} take place in addition to that at the interface of pentacene/C_{60}. In contrast, in the device with 6 nm-thick ZnPc layer, no contribution of pentacene in η_{EQE} suggests that pentacene layer is completely covered by ZnPc layer. Based on these results, the enhancement of η_p is attributed to the MCS interfaces where 2-nm-thick ZnPc on pentacene layer is responsible to increases V_{oc} and J_{sc}. The enhancement of V_{oc} can be attributed to the enhanced energy difference between HOMO of p-type material and LUMO of n-type material.[5,16,17] The enhanced J_{sc} is attributed to the additional η_{EQE} in 700 - 800 nm region originated from ZnPc layer.

On contrary, an insertion of ZnPc layer thicker than 3 nm results in a decrease in J_{sc}. Since the insertion of thick ZnPc layer diminished the contribution of pentacene in the photocurrent action spectra [Fig. 2(a)], the exciton in pentacene with long exciton diffusion length (~65 nm)[4] can not reach at C_{60} layer. In this situation, pentacene layer does not contribute to charge generation but still acts as a hole transporting layer. In

other word, the devices with ZnPc layer thicker than 3 nm mainly reflects charge separation characteristics at ZnPc/C_{60} interface. Based on this consideration, we will discuss the reason for the decrease in J_{sc} below.

The overlap of η_{EQE} with the solar spectrum determine the amount of J_{sc}. The η_{EQE} is expressed in $\eta_{EQE}=\eta_A\times\eta_{ED}\times\eta_{CT}\times\eta_{CC}$, where η_A is the absorption efficiency, η_{ED} is the exciton diffusion efficiency, η_{CT} is exciton dissociation efficiency at the charge separation interface and η_{CC} is the carrier collection efficiency.[3] Among the factors determining η_{EQE}, η_A, η_{ED}, and η_{CC} may not play major role in the decrease in η_{EQE} with increasing the thickness of ZnPc layer. Because, η_A should be improved as increasing ZnPc thickness, η_{ED} would be unchanged since the thickness of ZnPc layer is always less than exciton diffusion length of ZnPc (30 nm)[3,6] and η_{CC} should be the same since electrode metal is unchanged. Having considered these, we concluded lower J_{sc} would be due to low exciton dissociation efficiency (η_{CT}) at ZnPc/C_{60} interface compared with that of pentacene/C_{60} interface. Smaller η_{CT} in ZnPc/C_{60} may be related to that lifetime of singlet excited state of ZnPc (3.3 ns)[19] is shorter than that of pentacene (19 ns).[20] Thus, the reason why J_{sc} decreases by insertion of ZnPc layer thicker than 3 nm is that the area of pentacene/C_{60} interface with higher η_{CT} decreased with increasing that of ZnPc/C_{60} interface with lower η_{CT}.

Fill factor (FF) is another component parameter to determine η_P in addition to J_{sc} and V_{oc}. In the Fig. 2(d), FF is constant in the range from 0- to 6-nm-thick ZnPc, while FF of the device with 10 nm ZnPc decrease drastically. These results can be explained by R_s and R_{sh} of the devices. When R_s increases, J_{sc} may decrease without remarkable change of the V_{oc}. On the other hand, if R_{sh} tends to decrease, V_{oc} may decrease without remarkable change of the J_{sc}.[21] To obtain a high fill factor for efficient η_p, R_s

approaching zero and R_{sh} approaching infinity is desirable. Table 1 shows R_sA and $R_{sh}A$ as a function of the film thickness of ZnPc, where A indicates device area (0.04 cm^2). R_s and R_{sh} would be primarily determined by bulk resistance of organic layer and leakage current through organic layer, respectively. Root mean square (RMS) factors and Peak to Valley of the surface of ZnPc (x nm)/pentacene (50 nm) on ITO substrate were measured with atomic force microscope (AFM). R_sA and $R_{sh}A$ were estimated from the inverse slopes of the forward and reverse characteristics, respectively.[18,22] R_sA increased with increasing film thickness ZnPc, which is due to lower hole mobility of ZnPc compared with that of pentacene.[23] On the other hand, $R_{sh}A$ increased with increasing film thickness of ZnPc. This is because the surface roughness on the pentacene film becomes small with increasing film thickness ZnPc (Table 1). Based on these results, FF of the 2-nm-thick device giving highest η_P does not change compared with the device without ZnPc since increase of R_sA and $R_{sh}A$ are canceled each other. In contrast, FF of the device with 10 nm ZnPc decreases compared with that of the device without ZnPc. This is due to increase of R_sA. Indeed, by replacing thin film of ZnPc with higher hole mobility compound CuPc,[24] FF increased gradually as a function of film thickness of CuPc (data not shown). In the case of CuPc, $R_{sh}A$ increased with increasing CuPc thickness without prominent increase of R_sA.

4. Conclusions

In conclusion, we demonstrate the organic photovoltaic cells with MCS interfaces composed of pentacene/C_{60} and ZnPc/C_{60}. By inserting thin layer of ZnPc layer (~2 nm), we can control *V*oc and J_{sc} independently. The maximum η_P attains 2.07% in ITO/pentacene (50 nm)/ZnPc (2 nm)/C_{60} (40 nm)/BCP (10 nm)/Ag (100 nm) and the

enhancement is largely attributable to the MCS interfaces. In addition, we have pointed out the correlation between FF and surface roughness at charge separation interface. The MCS interface will provide new device architecture for the development of efficient organic solar cells.

References

1. C. W. Tang: Appl. Phys. Lett. **48** (1986) 183.
2. P. Peumans and S. R. Forrest: Appl. Phys. Lett. **79** (2001) 126.
3. P. Peumans, A. Yakimov, and S. R. Forrest: J. Appl. Phys. **93** (2003) 3693.
4. S. Yoo, B. Domercq, and B. Kippelen: Appl. Phys. Lett. **85** (2004) 5427.
5. G. P. Kushto, W. Kim, and Z. H. Kafafi: Appl. Phys. Lett. **86** (2005) 093502.
6. Y. Shao and Y. Yang: Adv. Mater. **17** (2005) 2841.
7. C. Chu, Y. Shao, V. Shrotriya, and Y. Yang: Appl. Phys. Lett. **86** (2005) 243506-1.
8. F. Padinger, R. S. Rittberger, and N. S. Sariciftci: Adv. Funct. Mater. **13** (2003) 85.
9. W. Ma, C. Yang, X. Gong, K. Lee, and A. J. Heeger: Adv. Funct. Mater. **15** (2005) 1617.
10. A. K. Pandey, S. D. Seignon, and J. M. Nunzi: Appl. Phys. Lett. **89** (2006) 113506-1.
11. M. Hiramoto, H. Fujiwara, and M. Yokoyama: Appl. Phys. Lett. **58** (1991) 1062.
12. P. Peumans, S. Uchida, and S. R. Forrest: Nature **425** (2003) 158.
13. F. Yang, M. Shtein, and S. R. Forrest: Nat. Mater. **4** (2005) 37.
14. A. Kahn, N. Koch, and W. Gao: J. Polym. Sci., Part B **41** (2003) 2529.
15. V. Djara and J.C. Bernède: Thin Solid Films **493** (2005) 273.
16. A. Gadisa, M. Svensson, M. R. Andersson, and O. Inganäs: Appl. Phys. Lett. **84** (2004) 1609.
17. K. L. Mutolo, E. I. Mayo, B. P. Rand, S. R. Forrest, and M. E. Thompson: J. Am. Chem. Soc. **128** (2006) 8108.
18. S. Yoo, B. Domercq, and B. Kippelen: J. Appl. Phys. **97** (2005) 103706.

19. D. M. Guldi, I. Zilbermann, A. Gouloumis, P. Vázquez, and T. Torres: J. Phys. Chem. **108** (2004) 18485.
20. T. C. Chang and D. D. Dlott: J. Chem. Phys. **90** (1989) 3590.
21. Y. Hamakawa and Y. Kuwano: *Taiyo Enerugi Kogaku* (Solar Energy Engineering) (Baifukan, Tokyo, 1994) p. 26 [in Japanese].
22. C. Waldauf, M. C. Scharber, P. Schilinsky, J. A. Hauch, and C. J. Brabec: J. Appl. Phys. **99** (2006) 104503.
23. C. D. Dimitrakopoulos and P. R. L. Malenfant: Adv. Mater. **14** (2002) 99.
24. Y. Terao, H. Sasabe, and C. Adachi: Ext. Abstr. (53nd Spring Meet., 2006); Japan Society of Applied Physics and Related Societies, 23a-S-6 [in Japanese].

Explanation of Figure

Figure 1. Illustration of the device structure with multi charge separation interface and the model of multi charge separation interface.

Figure 2. (a) J-V characteristics of ITO/pentacene (50 nm)/ ZnPc (x nm)/C_{60} (40 nm)/BCP (10 nm)/Ag (100 nm) under simulated AM1.5 solar illumination. (b) Energy diagram of the device used in this study. (c) plots of J_{sc} and V_{oc} as a function of the thickness of CuPc. (d) plots of η_P and FF as a function of the film thickness of ZnPc.

Figure 3. (a) η_{EQE} spectra as a function of the thickness of ZnPc film. (b) Absorption spectra of the films of pentacene, ZnPc and C_{60}. The film thickness of all samples is 50 nm.

Table 1. RMS and peak to valley of the surface of ZnPc (x nm)/pentacene (50 nm) on ITO substrate in addition to FF, R_s, and R_{sh} of ITO/pentacene (50 nm)/ ZnPc (x nm)/C_{60} (40 nm)/BCP (10 nm)/Ag (100 nm).

ZnPc film thickness (nm)	RMS (nm)	Peak to valley (nm)	FF	R_sA (Ωcm^2)	$R_{sh}A$ (Ωcm^2)
0	6.7±0.3	29.2±1.9	0.56	1.9 ±1.2	7741 ±1000
2	6.0±0.2	23.4±1.8	0.56	2.1 ±0.1	40375 ±7000
6	5.4±0.1	19.3±1.2	0.54	2.1 ±0.1	82390 ±20000
10	5.2±0.1	18.7±1.8	0.45	2.8 ±0.5	110902 ±8200

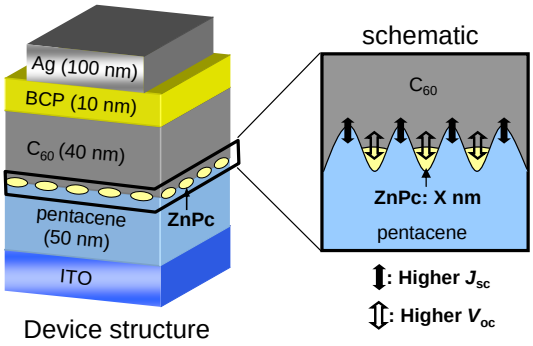

Fig. 1

Y. Kinoshita et al.

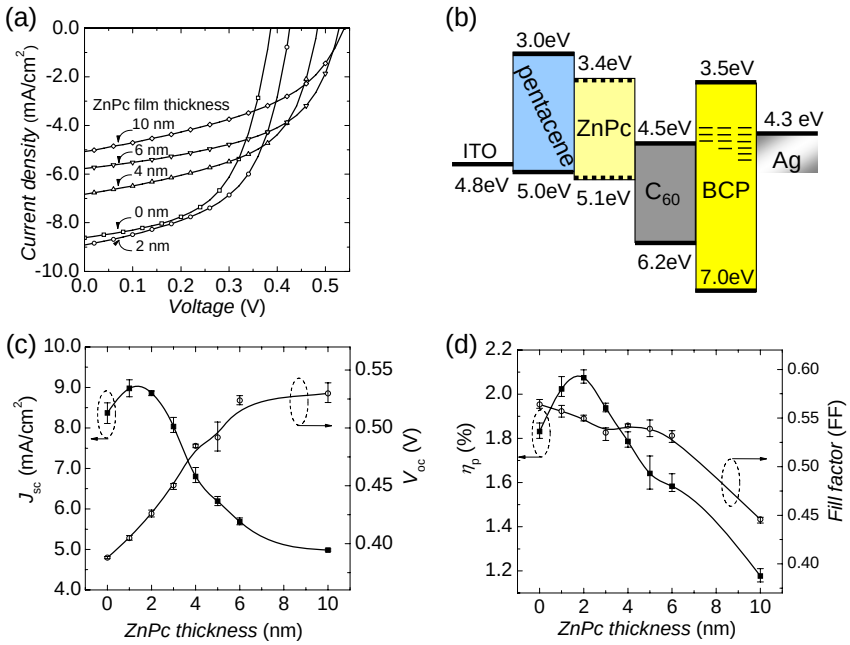

Fig. 2

Y. Kinoshita et al.

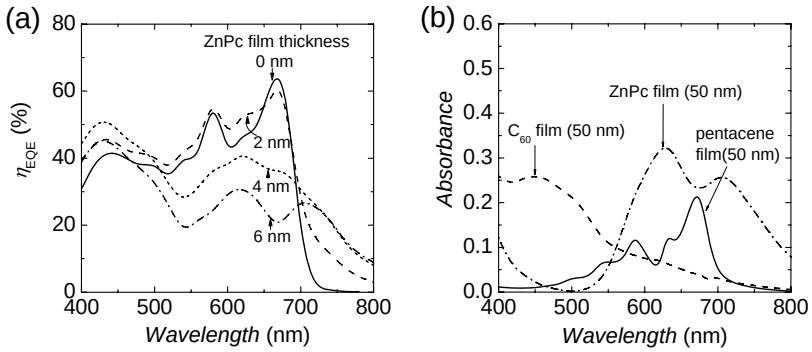
(a)
ZnPc film thickness
0 nm
2 nm
4 nm
6 nm
η_{EQE} (%)
Wavelength (nm)
(b)
Absorbance
ZnPc film (50 nm)
C_{60} film (50 nm)
pentacene film(50 nm)
Wavelength (nm)

Fig. 3